II WORKSHOP DE APLICAÇÕES
DE TÉCNICAS ELETROMAGNÉTICAS
PARA O MONITORAMENTO AMBIENTAL

Frequency-Dependent Permittivity for Soil Water Content Determination

Prof. Dr. Scott Jones, PSB/USU – UTAH/EUA

Scott B. Jones, Assistant Professor, Utah State University

Ricardo Estevez-Mejia, Undergraduate Student, Utah State University

David A. Robinson, Senior Lecturer, University of West Indies, Trinidad and Tobago

Jones, S.B., R. Estevez-Mejia and D.A. Robinson. 2008. Frequency-Dependent Permittivity for Soil Water Content Determination. ***Second workshop for applications of electromagnetic techniques in environmental monitoring.*** August 26-27, 2008. Department of Civil Engineering – University of Taubate (UNITAU), Brazil.

Contents

List of Figures

Abstract

Dielectric permittivity measurements have been used for decades to infer water content of soil and other porous media due to the large contrast in permittivity between water (80) and other soil constituents (1 to 10). Time domain reflectometry (TDR) has been the standard measurement for soil due to its excellent accuracy and ability to determine bulk electrical conductivity simultaneously. Unfortunately, measurements in the time domain yield only a single permittivity value associated with an unknown frequency. Additional soil property information can be extracted from frequency spectra of soil permittivity. associated with soil texture (surface area) and sources of electrical (EC) and dielectric loss. A bench top network analyzer and commercial dielectric probe were referenced for complex permittivity measurements in a range of dielectric liquid mixtures. We constructed and tested several flange-type open-ended dielectric probes using readily available coaxial adapters. A portable network analyzer, selected for its in-field measurement ability, was used for evaluating probe quality and validating probe-measured frequency-dependent permittivity in the reference dielectric liquids. Bilinear analysis was used to convert the measured reflection coefficients to complex permittivity spectra. Permittivity determinations of liquid dielectrics show excellent correlation to reference measurements using bilinear analysis. A pressure cell was constructed to facilitate permittivity determinations in a silt loam soil across a range of

water contents during drainage. Measurements in the silt loam soil show relaxation occurring throughout the measured frequency range (20 to 6000 MHz) with increased dielectric enhancement below 100 MHz likely due to Maxwell Wagner effects. Except for the saturated measurement, the resulting range of frequency-dependent permittivities yielded volumetric water contents (based on conventional assessment) greater than bulk sample water contents determined from oven-drying and mass balance calculations. Additional effort is needed to identify relationships between volumetric water content and variable measurement frequency and the soil-specific properties associated with relaxation phenomena. Ongoing work is looking into the possibility of using this technique for on-the-go measurement of water content for field-scale mapping purposes.

1. Introduction

Water content is a critical variable of interest in agriculture, manufacturing, food production, pharmaceuticals, and a long list of disciplines whose products contain water. The high dielectric permittivity of water relative to other substances provides a contrast that yields excellent measurement resolution with more than an order of magnitude difference in the permittivity of constituents such as solid minerals, air, and organic matter compared to that of water. Electromagnetic measurements in soil began as early as 1933, with radio-frequency determinations followed by decades of

frequency-domain measurements [*Smith-Rose*, 1933] (Smith-Rose, 1933; Scott et al., 1967; Hoekstra and Delaney, 1974). Smith-Rose explained the increase in dielectric constant measured at reduced frequencies as arising from polarization effects due to electrolytic conduction. Figure 1 illustrates the relaxation phenomena associated with a range of contributors extending from ion polarization, to molecular rotation to atomic and electronic effects. The water molecule is dipolar and a significant energy storage resource (dielectric) under an applied electromagnetic field and is the basis of water content measurements in soil.

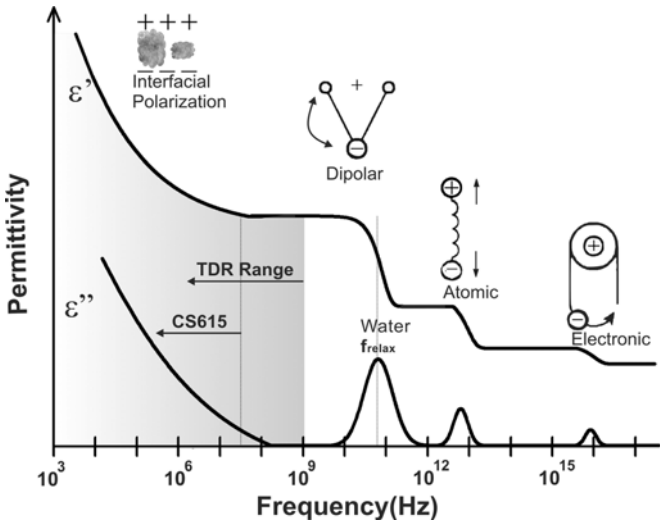

Figure 1. Frequency-dependent real and imaginary permittivities illustrating interfacial polarization and dipolar relaxation effects that occur within the range of electromagnetic measurements used in soils [*Chen and Or*, 2006].

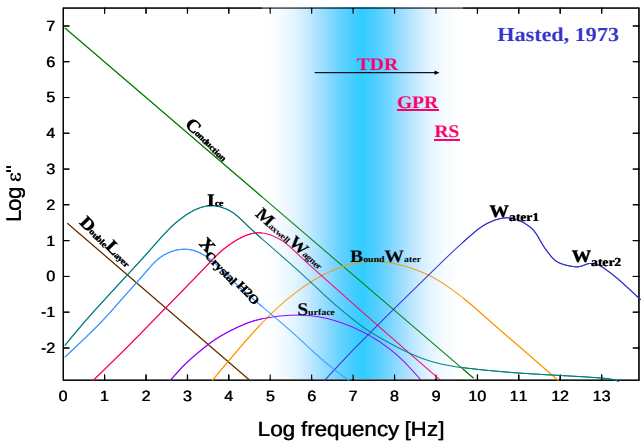

Figure 2. Relaxation mechanisms shown as a function of frequency [*Hasted*, 1973]. The frequency measurement range of Time domain reflectometry (TDR), ground penetrating radar (GPR) and remote sensing (RS) techniques are indicated.

1.1 Frequency-dependent factors

The advantage of measuring water content via permittivity in the frequency-domain is highlighted by the opportunity to observe relaxation effects associated with soil texture and soil constituents. Figure 2 illustrates the frequency-dependent magnitude of contributors to dielectric energy loss. For typical electromagnetic measurement devices operating in the MHz to GHz frequency range, the major contributors include Maxwell Wagner-, ionic conduction- and bound water-effects.

Soils, especially those with high clay and organic matter content, show appreciable dielectric dispersion, *i.e.* the real permittivity changes as a function of frequency. This means that the real (ε') and imaginary (ε'') parts of the permittivity describing energy storage and energy losses, respectively, change as a function of frequency. Figure 3 illustrates permittivity measurements in soil minerals where it is apparent that some are more susceptible to relaxation effects than others. Quartz sand, which has a relatively low surface area compared to clays, shows relatively little relaxation in a nearly saturated state. Talc shows a similar trend but with slightly more relaxation below 100 MHz. The sodium bentonite clay in a dry state, exhibits slightly more relaxation, but when mildly wetted, the clay permittivity increases dramatically at reduced frequencies. The relaxation phenomenon may therefore be useful as an indicator of soil texture or surface area. When permittivity measurements are coupled with electrical conductivity measurements, the impact of ions on relaxation phenomena such as Maxwell-Wagner effects may become more evident.

To illustrate this, we cite the work of Chen and Or (2006) where they compared real permittivity measurements in the frequency domain shown in Figure 4a. Frequency-dependent permittivity was highly variable below 100 MHz, increasing with increasing solution electrical conductivity and reduced frequency. Above 100 MHz, the permittivity was unchanged by ions in solution, yielding a more reliable measurement of permittivity for water content determination. The enhancement in permittivity below several hundred MHz, was attributed to Maxwell Wagner relaxation in this sand.

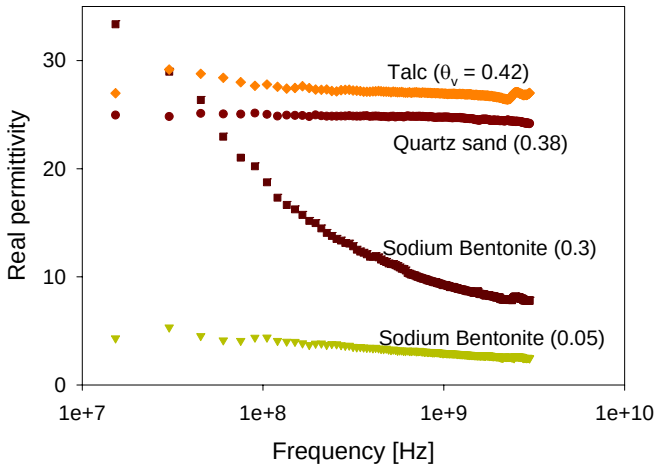

Figure 3. Real and imaginary components of relative permittivity as function of frequency for ice and water with EM sensors and measurement techniques listed.

The use of time-domain reflectometry (TDR) in soil was inspired by the seminal work of Topp, Davis and Annan [1980]. Advantages of the TDR technique include the simultaneous determination of water content and electrical conductivity; however, high equipment costs inspired development of EM-based sensors using capacitance- and inductance-techniques. With each of these approaches, the permittivity value derived was either associated with the frequency of the measurement device or the frequency of measurement was broadband resulting in an unknown effective measurement

frequency (Robinson et al., 2006). Figure 4b shows waveforms derived from TDR measurements in the same sand as Figure 4a. The constant travel time shown in Figure 4b demonstrates that TDR is not influenced by the electrical conductivity of the porous media for moderate levels of EC. It also indicates the effective frequency of the TDR is much higher than a few hundred MHz, yielding a permittivity that is unchanged by the soil salinity in this case. So while TDR provides both a measure of permittivity and electrical conductivity, the effective measurement frequency remains unknown. The significant advantage of permittivity measurements made in the frequency domain is the ability to observe relaxation effects and select a reference frequency to standardize measurements.

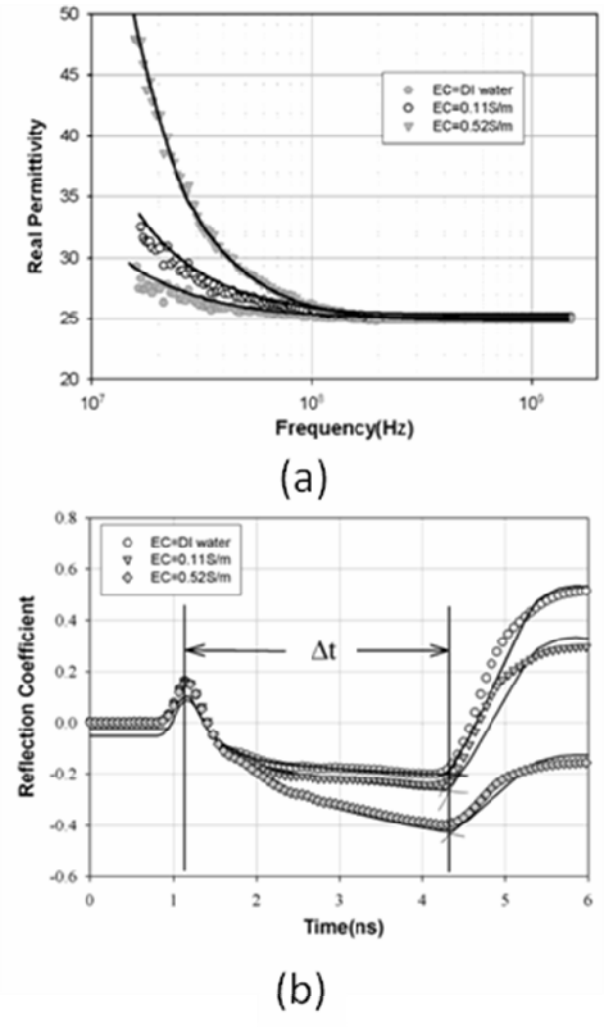

Figure 4. a) Illustration of constant permittivity obtained in saturated Ottawa sand at frequencies above a few hundred MHz where effects from ion polarization or Maxwell Wagner Effects are diminished [*Chen and Or*, 2006]. b) Time domain reflectometry (TDR) waveforms illustrating the constant travel time obtained in soil of varying electrical conductivity.

1.2 Electromagnetic Sensors and Measurements

After TDR measurement systems were developed, a number of smaller, less expensive dielectric-based sensors were developed for water content determination. Some of these probes and techniques were evaluated using a standardized comparison in dielectric liquids rather than soils [*Blonquist et al.*, 2005; *Bogena et al.*, 2007; *Jones et al.*, 2005]. Figure 5 shows a representative illustration of the reduction in measurement root mean squared error (RMSE) associated with increasing measurement frequency. Some of this effect is associated with the quality and therefore expense of the instrument/sensor where price generally increases with increasing frequency. Cellular phone technology has created much less expensive components making it possible to make TDR quality sensors for several hundred dollars. The TDR bandwidth ranges across the frequency band up to 1.5 GHz, while certain sensors are rated at fixed frequencies (Echo @ 5 MHz, Hydra @ 50 MHz and Theta @ 100 MHz). Because of the large contrast between the permittivity of water (80 in the 100-1000 MHz frequency range) and those of the soil minerals (5-8) and air (1), the soil permittivity is very sensitive to its volumetric water content, θ. Furthermore, the $\varepsilon_a(\theta)$ relationship is relatively universal and does not differ much from one agricultural soil type to another. The volumetric water content can be determined from apparent permittivity measurements using capacitance- or inductance-based techniques in addition to travel-time analyses

Considering the optimal measurement frequency in soils, indications are that between 300 and 5000 MHz provide less error associated with lossy soils (i.e., clayey or saline). Figure 5 illustrates the frequency dependence of some commonly used EM sensors with lower frequency sensors exhibiting greater measurement error than those operating at higher frequencies, such as TDR instruments.

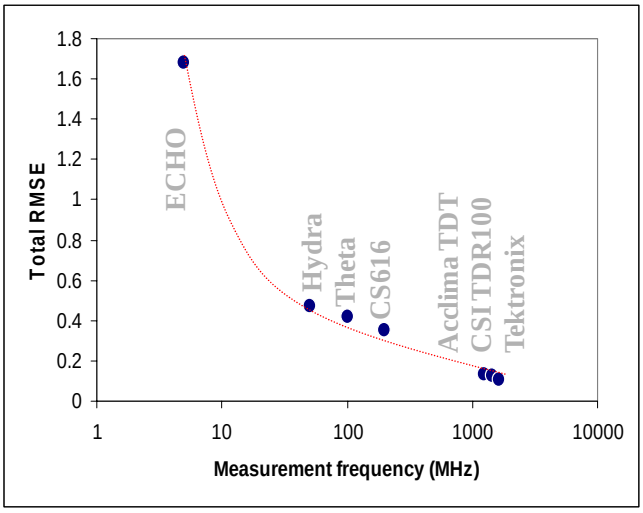

Figure 5. Root mean square error of measurements made by different electromagnetic sensors as a function of frequency (Blonquist et al., 2006) Measurements included losses from electrical conduction and dielectric dispersion in different liquids.

The primary objectives of this effort were to design, construct, and characterize an electromagnetic-based sensor providing frequency-dependent permittivity for soil water content determination. The sensor is designed to target optimal measurement frequencies in the range of a few hundred to a few thousand MHz based on low and high frequency constraints.

In order to overcome the difficulties of making measurements in soils and to minimize friction resistance of probes traveling through soil, a second option was to construct an open-ended probe. This approach relies on time domain reflectometry, in

which we adapted existing designs and interpretation algorithms. Open-ended probes have been widely used in physics and chemistry for permittivity measurements in liquids and biological tissue. Due to their small sampling volume and associated complex signal analysis, however, these probes have not been extensively used in soil measurement, but open-ended probes have excellent potential for on-the-go subsurface measurements [*Jones et al.*, 2006]. A major advantage is the minimal path length and subsequent low attenuation from electrical conduction. In soils with appreciable salinity, conventional time domain analysis with longer probes becomes progressively inaccurate due to signal attenuation to the point of failure. Recent research has demonstrated that permittivity, which is inextricable using TDR travel-time analysis in saline soils, could be extracted using frequency domain techniques and shorter TDR probes that reduce signal attenuation [*Jones and Or*, 2004].

The design, construction, and testing of an open-ended dielectric probe for water content determination was accomplished. This preliminary sensor is robust, compact and low cost; with a wide range of applications such as hydrological modeling, agricultural water management, and most studies of the soil. A bilinear analysis developed to characterize the relationship between the sensor output and the permittivity of the measurement under test yielded excellent correlation with the reference permittivity spectra of the liquids measured. Also, extending the bilinear

analysis to soil moisture determination showed good agreement with expected values in the range of 0.2 to 2 GHz.

2. Theoretical Considerations

There is an increasing interest in the application of the open-ended probe coaxial line for convenient and non-intrusive complex permittivity measurements of lossy materials at RF and Microwave frequencies; determination of the reflection coefficient at the sensor discontinuity plane allows one to derive the complex permittivity of a liquid, semi-solid, or soil sample terminating line [*Grant et al.*, 1989]. The measurement configuration of the coaxial line sensor with ground plane is shown in Figure 6.

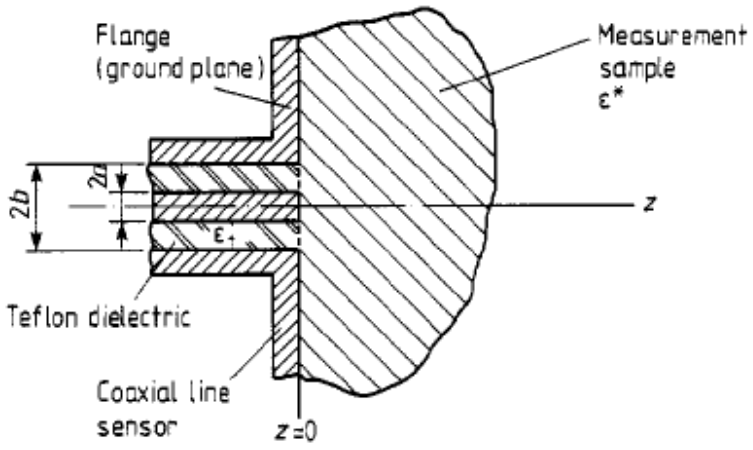

Figure 6: Open circuit coaxial line sample measurement configuration.

Open-ended coaxial probes have been studied extensively in order to measure the dielectric constant and dielectric loss factor at microwave frequencies. The sensor is placed in contact with the sample and its complex reflection coefficient *K* is measured. The main problem involving measurements with open-ended coaxial probes is that there exists no analytical relationship between the reflection coefficient and the permittivity. Several approximate models have been developed in the past and considerable efforts are being made to further improve these models. Faced with these theoretical models, the engineer who is concerned with the practical setup not only has to determine which model is suitable or sufficient for his needs, but he also has to determine the dimensions of the probe to be used and the size of the test sample [*De Langhe et al.*, 1994].

In the past, increasingly sophisticated models were found to model open-ended coaxial probes. Most of these models give an expression for the admittance as a function of the dielectric constant. Three different stages can clearly be distinguished in the experimental use of the coaxial probe. First, the lumped parameter model was introduced. The relative simplicity of this model allows a rapid inversion from the measured reflection coefficient to the dielectric constant. The second model is based on rigorous solutions of the electromagnetic field equations appropriated for a coaxial line open to dielectric sample. The third method employs an empirical relationship between the permittivity and the reflection coefficient called bilinear analysis.

2.1 Lumped Parameter Model

A method of calculating the complex permittivity that has the advantage of yielding simple closed-form equations is based on a model of the discontinuity at the termination of the coaxial line as an equivalent lumped circuit. This discontinuity, in the absence of a lossy dielectric, is frequently assumed to be purely capacitive and to consist of fields fringing both within the sensor's dielectric and out in the sample material terminating the line. The sensor discontinuity is then modeled as a lumped admittance with capacitances originating from fringing field (Ct) and sample fringing field (Cs), as shown in Figure 7 .

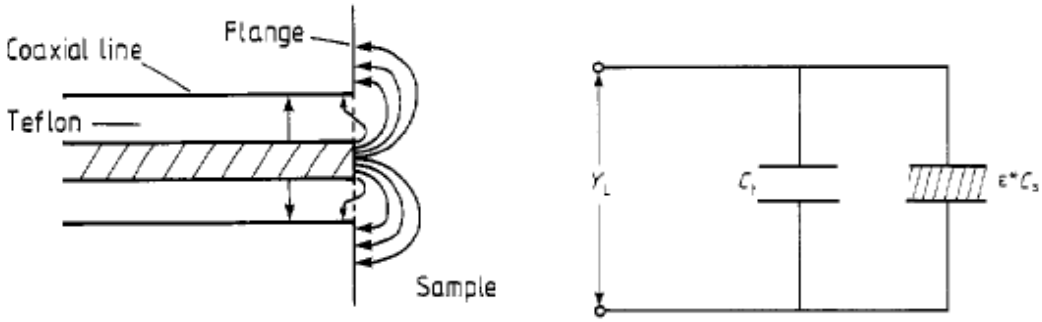

Figure 7: a) Coaxial line termination fringing fields and b) Sensor lumped equivalent circuit

This equivalent circuit is valid at frequencies where the dimensions of the line are small compared with the wavelength, so that the open end of the line is not radiating and all the energy is concentrated in the fringe or reactive near field of the line. At higher

frequencies, the value of the capacitance C_s increases with frequency, due to the increase in the evanescent TM modes being excited at the junction discontinuity

The reflection coefficient at the end of an open-ended probe in contact with a dielectric medium with relative permittivity ε^x and the load admittance, Y_L, are related through equation (1)

$$Y_L = Y_0 * \frac{1-\Gamma}{1+\Gamma} \tag{1}$$

where Y_0 is the characteristic impedance of the coaxial transmission line and Γ is the complex reflection coefficient.

The permittivity dependence of the admittance can be described as:

$$Y_L = j\omega C_p + j\omega(\varepsilon' - j\varepsilon'')C_s \tag{2}$$

where ω is the angular frequency, C_p is the fringing capacitance in the probe and C_s is the fringing capacitance into sample.

Combining equations (3) and (4), we obtain

$$\varepsilon' = \frac{-2 * |\Gamma| * \sin\theta}{\omega C_s Z_o(1 + 2 * |\Gamma| * \cos\theta + \Gamma^2} - \frac{C_p}{C_s} \tag{3}$$

and

$$\varepsilon'' = \frac{1 - |\Gamma|^2}{\omega C_s Z_o (1 + 2 * |\Gamma| * \cos\theta + \Gamma^2} \quad (4)$$

where ε' is the real part of the permittivity, ε'' is the imaginary part, Z_0 is the characteristic impedance of the transmission line and Γ is the magnitude of the complex reflection coefficient with angle θ.

In this form, C_p and C_s can be found from the gradient and ordinate intersection, respectively, of plotted data of the reflection coefficients of 'known' dielectric reference materials. The equivalent circuit model is valid providing (i) C_p and C_s, are independent of sample complex permittivity: (ii) C_p and C_s are independent of frequency and (iii) the probe does not launch propagating radiation (*i.e.* it does not behave as an antenna) [*Stuchly M. A.*, 1982].

2.2 Bilinear Analysis Model

2.2.1 Time Domain

For a dielectric measurement cell based on a coaxial-line geometry the relationship of an unknown admittance, y_x, and sample admittance, y_s, is conveniently written as [*Cole*, 1983]:

$$y_x - y_s = \frac{A^* \rho_x^* + C^*}{1 - B^* \rho_x^*} \tag{5}$$

where ρ_x^* is the reflection coefficient defined by:

$$\rho_x^* = \frac{v_0 - r_x}{v_0 + r_x} \tag{6}$$

The ideal response from a terminating dielectric (of thickness d) referenced against an ideal open circuit is also given by Cole [1983] as:

$$y_x = i\left(\frac{\omega \gamma d}{c}\right) \cdot \varepsilon_x^* \frac{\tan(z_x^*)}{z_x^*} \tag{7}$$

and d is the thickness of the dielectric sample, γ is the ratio of the actual air line admittance to the characteristic line admittance, c is the speed of light and ε_x^* is the complex permittivity. Cole [1983] described the relationship between the admittance and the relative sample permittivity ε_x^* using a power series expansion of Eq. (8) as:

$$y_x = i\left(\frac{\omega \gamma d}{c}\right) * \varepsilon_x^* (1 + a z_x^{*2} + b z_x^{*4}) \tag{8}$$

where coefficient *"a"* and "*b*" can be determined empirically. Combining Eq. (8) and Eq. (7) we obtain:

$$y_x = i\left(\frac{\omega d}{c}\right)\cdot\frac{\varepsilon_x^*}{1-a*\left(\frac{\omega\gamma d}{c}\right)^2 * \varepsilon_x^*} \tag{9}$$

Because Eq. (5) is bilinear in y_x we can solve in terms of ε_x^* by substituting Eq. (9) into Eq. (5) with the resulting expression written in terms of bilinear coefficients [*Cole et al.,* 1989].

$$\varepsilon_x^* = \frac{(1+A^*)\rho_x^* + C}{1-B^*\rho_x^*} \tag{10}$$

2.2.2 Frequency Domain

To simplify data processing, the signals are transformed to the frequency domain using numerical Fourier transformation Eq. (10) can be reduced to the following [*Berberian,* 1993]:

$$\varepsilon_x^* = \frac{A^*(\omega)\rho_x^*(\omega) + C(\omega)}{1-B^*(\omega)\rho_x^*(\omega)} \tag{11}$$

where ρ_x^* is now define as:

$$\rho_x^*(\omega) = \frac{(V_0(\omega) - R_x(\omega))}{(V_0(\omega) + R_x(\omega))} \tag{12}$$

This generalization of equation (11) provides a method for correcting effects of wave propagation and residual reflections using reference permittivity measurements.

Parameters A and B depend on the choice of the reference dielectric, admittance of the transmission line and connectors, and on the measurement system. The bilinear coefficients are determined by simultaneous solution of two equations deriving frequency-dependent permittivity and reflection coefficients from measurement in two calibration fluids of known permittivity. These parameters are computed by calibration with three standards: a short circuit, an open circuit and 50 Ω terminations or by the use of three dielectric samples with known permittivity (e.g., liquids within the permittivity range of interest).

3. Materials and Methods

The open-ended coaxial probe is a cut-off section of a transmission line [*Sheen and Woodhead*, 1999]. The measurement is made by immersing the probe into a liquid or interfacing with the flat face of a solid (or powder) material. The EM field at the probe end "fringes" into the material and changes in contact with the material under test (MUT). The reflected signal (S11) can be measured and related to ε_r^*. A typical measurement system using a coaxial probe method consists of a network analyzer, a coaxial probe, and an analytic method to relate the reflection coefficient and the permittivity. Time domain reflectometry techniques have also been used by fast Fourier transformation of the TDR measurement to the frequency domain.

3.1 Open-ended Probe

The quality of the transmission line and probe impact the resulting frequency-dependent dielectric measurement. Poorly designed configurations may act as a low-pass filter, reducing the frequency spectra of the measurement. While the calibration may remove some of the unwanted noise, the cable-probe interface should be a high quality connection.

3.1.1 Coaxial Adapters as Dielectric Probe Fixtures

Based on the design of an open-ended dielectric probe (i.e., Hewlett Packard 85070b), we considered a number of coaxial adapters and a tee for dielectric probe measurements (Figure 8). The open-ended probes were constructed using an N to UHF adapter (MxF), an N-type (FxF) hermetically sealed bulk head adapter, an SMA to TNC (FxF) adapter and a BNC Tee (MxFxM) for evaluation of two-sided measurements. Critical to obtaining a quality short circuit is having the end highly polished to provide a flat and smooth surface to contact the shorting block. This was accomplished by machining the end flat on a lathe, then hand sanding on a flat surface using successively finer grit sand paper beginning with 600, 1000, 1500 and finishing with 2000. Use of different fixtures was for evaluating the quality of measurement available from these differently sized measurement surface and to determine the frequency measurement spectrum available. The N-type connector is a high performance RF coaxial connector. This connector is able to withstand relatively high power when compared to the BNC or TNC connectors. The standard versions are specified for operation up to 11 GHz, although precision versions are available for operation to 18GHz. N-type plugs are designed not only for the required impedance, but also to accept a particular coax cable format. In this way, all the internal parts are compatible with the coaxial cable used.

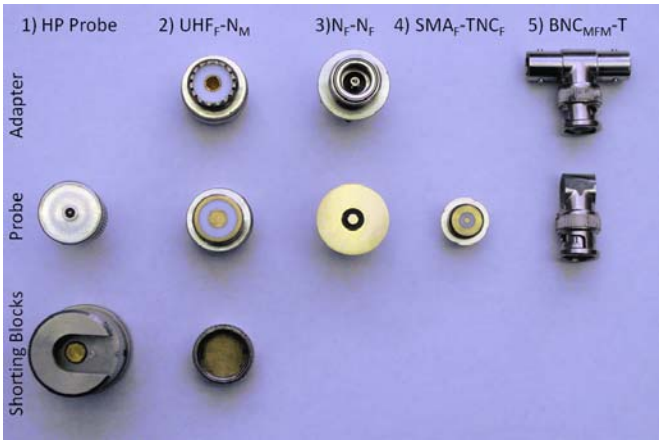

Figure 8. Coaxial adapters used to make dielectric probes. Probes were made from 1) a Hewlet Packard dielectric probe (HP 85070b), 2) an N to UHF adapter (MxF) 3) an N-type (FxF) hermetically sealed bulk head adapter, 4) an SMA to TNC (FxF) adapter and 5) a BNC Tee (MxFxM). Shorting blocks are shown for probes 1 and 2.

The UHF connector is a coaxial RF connector that is used in low-cost applications for frequencies often in the high frequency (HF) and the bottom end of the VHF spectrum. Although it does not offer a particularly high level of performance, this RF connector is nevertheless satisfactory for many applications where cost may be an issue. This RF connector design was aimed to cover frequencies in the range 0.6 to 300 MHz and it was aimed at use within the radio industry. This type of adapter was chosen to provide a large fringing field, as the UHF coaxial diameter is among the largest available and allows the engineers to avoid using extra adaptors between the probe and the Vector Network Analyzer (VNA). Another reason for the use of the UHF connector is that the end of this adapter has a greater area in contact with the sample than terminals such as N-type, SMA, BNC, mini UHF, or TNC.

3.1.2 HP Dielectric Probe Kit

The HP 85070B High-Temperature Dielectric Probe Kit (HP probe in Figure 8) was used as the permittivity standard measurement instrument. The probe was

attached to an HP 8752C network analyzer for measurement of real and imaginary permittivity using software provided by Hewlett Packard.

3.1.3 Low Loss Cables

An important feature to consider is the use of high quality (low loss) cable connecting the network analyzer and probe. The HP probe was interfaced with the HP NA using an air line with SMA connectors at each end. Flexure in the cable over the years had reduced the quality of this cable and we found excellent results using custom cables including LMR-400 which has considerably reduced loss compared to RG-58 or RG-8 (Figure 9). Cable losses are technically removed through calibration procedures, but if significant filtering occurs, this impacts the higher frequencies and causes anomalies in the measurements.

3.2 Vector Network Analyzer

3.2.1 HP Network Analyzer

A bench top HP 8752C Network Analyzer was used to measure and characterize the dielectric liquid standards used for characterization and calibration of probes and the bilinear analysis approach. The HP 85070E dielectric probe kit was used to measure complex permittivity of a range of liquids (mixtures of Isopropoxyethanol and water) to cover the range of dielectrics of interest. Before measuring, calibration at the tip of the probe must be performed. A three-term calibration corrects for the directivity, tracking, and source match errors that can be present in a reflection measurement. In order to solve for these three error terms, three well-known standards are measured. Calibration is carried out using an open circuit, a shorting block, and water. The calibration is computed internally using the HP Dielectric Probe Kit software (v 02.00, Agilent Technologies).

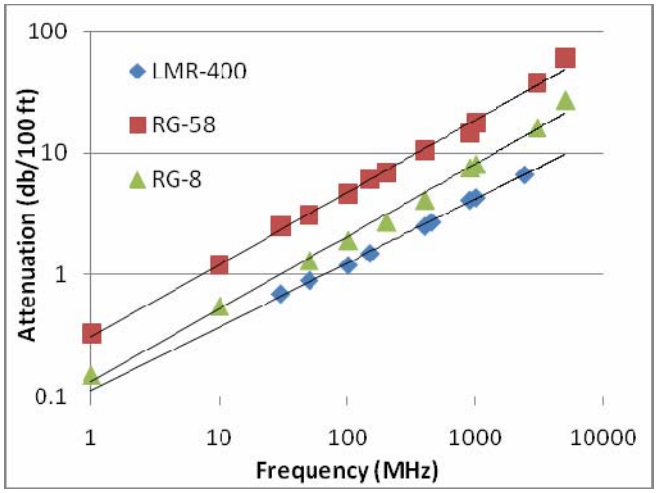

Figure 9. Attenuation in coaxial cable showing the reduced loss using LMR-400 compared to other common cables.

3.2.2 Anritsu Network Analyzer

A portable Anritsu MS2026A network analyzer (Figure 10, Anritsu Corp., www.anritsu.com) was also used to obtain raw scatter functions used in the bilinear analysis approach for dielectric measurements. The VNA scatter functions obtained

with the open-ended probes were measured between 2 MHz to 5 GHz . The Anritsu device is a 1- or 2-port handheld vector network analyzer (VNA), which uses Frequency Domain Reflectometry (FDR). Using FDR, the VNA Master provides 1-port measurements of return loss, VSWR, cable loss, Distance-To-Fault (DTF), and Smith Chart measurements in the field. The VNA offers measurement capabilities for S_{11} and S_{21} measurements in the field. This VNA was chosen because it was portable with state-of-the-art technology and could interface with a PC using the Anritsu Master Software Tools for Windows 2000/XP/Vista. The PC connection is a USB 2.0 (full-speed), Ethernet LAN, or Direct Ethernet interface.

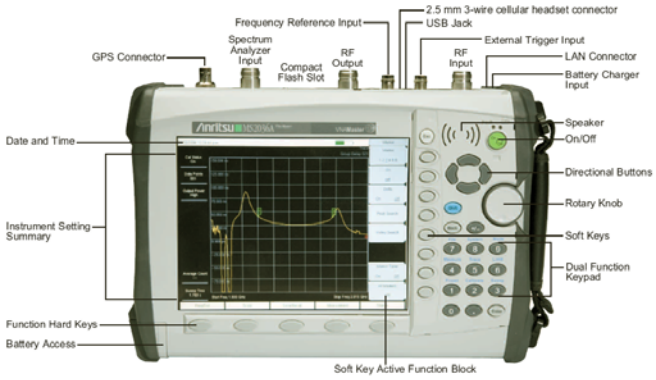

Figure 10. Anritsu (Richardson, TX) model MS2026A portable vector network analyzer (VNA) used for measurement and analysis of permittivity through bilinear analysis.

3.2.3 Calibration Liquids

Calibration liquids were chosen to provide a spectrum of permittivities for validation of the open-ended measurements. We chose Dioxane:water mixtures [*Bogena et al.*, 2007; *Schwank et al.*, 2006] and Isopropoxyethanol:water mixtures [Blonquist et al., 2005; Jones et al., 2005] as reference dielectrics due to their miscible nature and to their relatively high relaxation frequencies. These liquids have the advantage of providing a

permittivity range that can vary from ⊚r = 2.2 with pure Dioxane, ⊚r= 12.7 with pure Isopropoxyethanol and ⊚r =80 for pure water (see Table 1). The [*Cole and Cole*, 1941] parametric model was used to predict the complex permittivity of each measured liquid, given as:

$$\varepsilon^* = \left[\varepsilon_\infty + \frac{(\varepsilon_s - \varepsilon_\infty)}{1 + \left(\frac{j \cdot f}{f_{rel}} \right)^{1-\alpha}} \right] + \frac{j \cdot \sigma_{dc}}{2\pi \cdot f \cdot \varepsilon_0} \qquad (13)$$

where ε_s is the static permittivity, ε_∞ is the infinite (i.e. high frequency) permittivity, f is frequency [Hz], f_{rel} is the relaxation frequency [Hz], and α is a

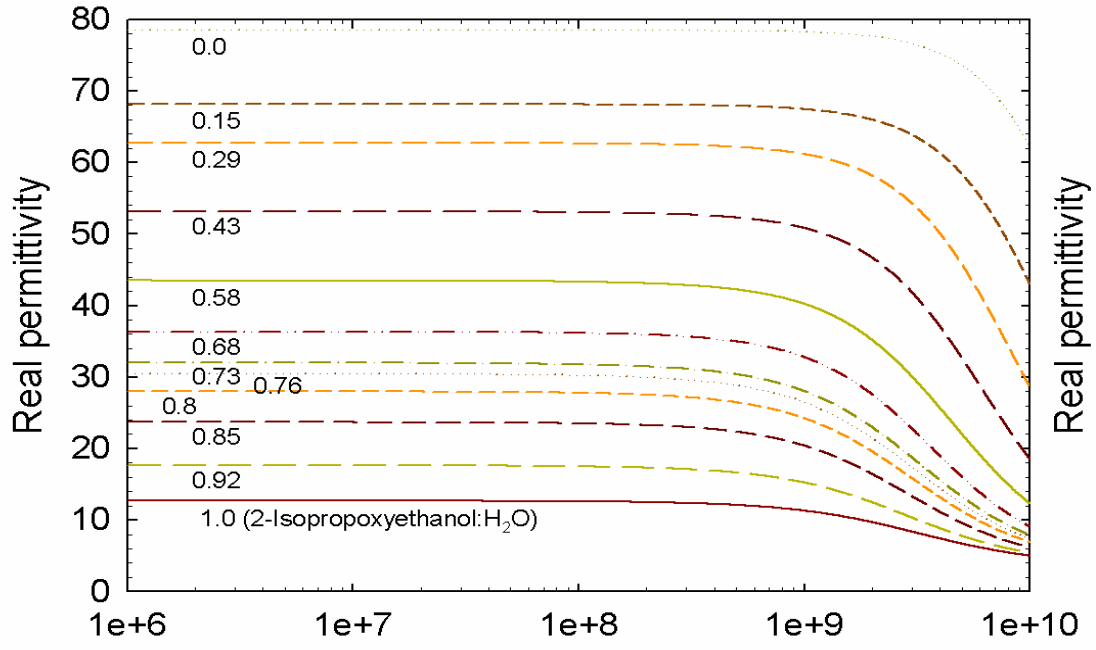

Figure 11. Real permittivity measured using the commercial HP dielectric probe in Isopropoxyethanol-water mixtures from [*Jones et al.*, 2005].

parameter that corresponds to the dispersion in the relaxation frequency range. Table 1 contains Cole-Cole parameters defined by [*Jones et al.*, 2005] that were fit to Dioxane- and Isopropoxyethanol-water mixtures. The isopropoxyethanol:water mixtures plotted in Figure 11 provide a family of uniform dielectric liquid permittivities across a frequency spectrum from 1 MHz up to around 500 MHz making these mixtures ideal for calibration and testing liquids. We used these modeled permittivities for characterization of the goodness of the portable network analyzer measurement capability when bilinear analysis was applied to dielectric measurements of the same liquids.

Table 1. Cole-Cole parameters (Eq.(13) fitted to network analyzer measurements in non-relaxing mixtures of Dioxane:water (D:W) and 2-isopropoxyethanol:water (I:W) and in relaxing dielectric liquids shown. Model parameters are ε_s, the static permittivity; ε_∞, the high frequency permittivity; f_{rel}, the relaxation frequency [Hz]; σ_b, the bulk electrical conductivity [S m^{-1}]; ε_0, the permittivity of free space ($8.854 \cdot 10^{-12}$ F m^{-1}) and α is a parameter ranging from 0 to 1 that corresponds to the dispersion in the relaxation frequency range.

	ε_s§	ε_∞	σ_b [dS m^{-1}]	f_{rel} [GHz]	α	RMSE (ε')	RMSE (ε'')
D:W = 1.000*	2.45	2.01	0.000	23.4	0.01	0.052	0.050
D:W = 0.962	3.62	2.01	0.00	19.9	0.02	0.054	0.049
D:W = 0.925	5.25	2.01	0.00	13.5	0.04	0.054	0.070
D:W = 0.890	6.99	2.01	0.00	12.2	0.07	0.054	0.061
D:W = 0.855	9.09	2.01	0.00	10.6	0.08	0.058	0.063
I:W = 1.000	12.70	3.50	0.00	3.25	0.12	0.142	0.163
D:W = 0.79	12.91	2.01	0.00	9.36	0.07	0.057	0.070
I:W = 0.920	17.65	3.50	0.00	2.87	0.11	0.115	0.183
I:W = 0.855	23.70	3.50	0.00	2.89	0.10	0.240	0.189
I:W = 0.800	28.00	3.50	0.00	3.03	0.10	0.213	0.146
I:W = 0.760	30.50	3.50	0.00	3.12	0.10	0.112	0.170
I:W = 0.727	32.00	3.50	0.00	3.28	0.10	0.142	0.180
I:W = 0.680	36.35	3.60	0.00	3.70	0.08	0.0972	0.155
I:W = 0.580	43.50	3.60	0.00	4.55	0.08	0.260	0.178
I:W = 0.430	53.15	3.60	0.00	6.12	0.06	0.179	0.263

I:W = 0.290	62.75	3.60	0.00	8.38	0.05	0.215	0.179
I:W = 0.150	68.15	3.60	0.00	12.7	0.03	0.275	0.249
di-water	78.50	4.50	0.00	18.7	0.00	0.0842	0.184
1-propanol	22.75	4.25	0.00	0.475	0.04	0.258	0.489

*ε_∞ for Dioxane = 2.01 [*Aralaguppi et al.,* 1996]

3.3 Measurement Methodology

Figure 12 shows the process taken to obtain a permittivity measurement using bilinear analysis and the vector network analyzer (VNA)-open-ended probe system. With the open-ended probe connected to the VNA, an open, short and load (water) are applied to the probe to calibrate the VNA-probe system. After calibration of the VNA, S_{11} measurements of calibration fluids are obtained. Examples include measurements in air, various alcohols or water being carried out in order to determine the bilinear coefficients A, B and C from known debye (or Cole-Cole) functions for these liquids. Once both the VNA-probe calibration and bilinear coefficients are determined, S_{11} measurements are taken of unknown materials with the VNA and exported and analyzed using mathematical software. Finally, the bilinear coefficients allow analysis of the unknown permittivity of liquids or soil.

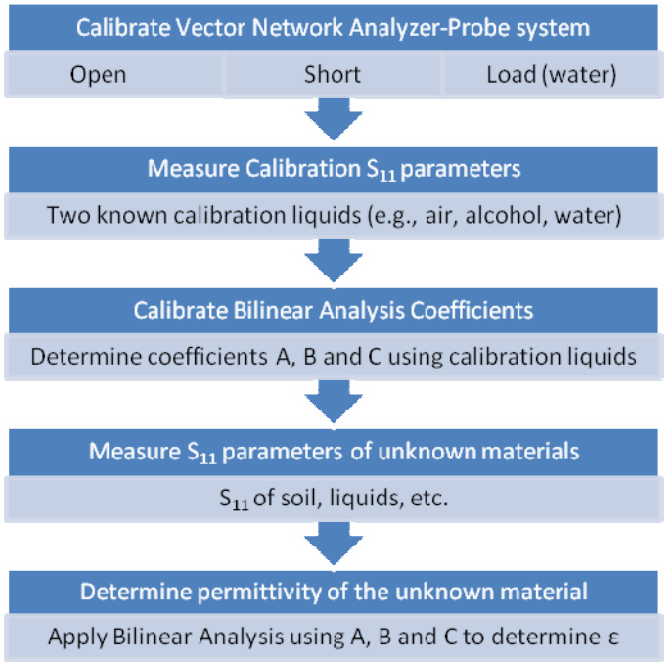

Figure 12. Outline of the process required for calibration of the VNA-probe system, generation of bilinear coefficients and subsequent analysis for permittivity determination.

3.4 Soil Test Apparatus

One of the challenges of measuring soil permittivity across a range of water contents is maintaining a consistent bulk density with uniform soil-probe contact. This is important because of the relatively small electromagnetic fringing field generated by the probe. In order to overcome these difficulties, a modified Tempe cell used for water retention measurements, was constructed to allow variably saturated soil measurements using the open-ended probe. A picture of the modified cell with the N-type open-

Figure 13. Modified Tempe cell designed to provide soil permittivity measurements to coincide with draining water retention measurements. Pressure was applied in steps to the cell to force water out the bottom through a ceramic plate. A water content sensor was also included in the cell for independent measurements of volumetric soil water content.

ended dielectric probe and a water content sensor (EC-5, Decagon Devices, Pulman, WA) for water content measurements is shown in Figure 13. The cell was packed to a bulk density of 1.35 g cm^{-3} with Millville Silt Loam soil (coarse-silty, carbonatic, mesic Typic Haploxeroll) from the Greenville Farm in Logan, Utah. The soil was previously sieved through a 1 mm screen and had a reported clay content of 18 percent. Pressure steps were applied beginning from saturation at 0, 1, 2, 4, 6, and 8 m of water head. At each pressure step, the sensor-determined measured water content was monitored until a quasi-equilibrium level was reached. Outflow water mass was tracked for independent calculation of soil volumetric water content and the final water content was determined from oven drying the soil after the final pressure step. The initial porosity was estimated by filling with dry soil to a predetermined volume. After wetting and subsequent drainage, shrinkage of the soil occurred estimated to be about 3 – 5 percent by volume. An ECHO EC-5 dielectric sensor was also installed in the cell for independent determination of water content change to determine establishment of equilibrium. The factory calibration was applied to the voltage output for estimation of water content.

4. Results and Discussion

4.1 Calibration of the Portable Network Analyzer

The VNA calibration process is one of the most important steps in order to ensure quality measurements. If the calibration is not performed appropriately, the final measurements will be compromised. A simple indicator for proper calibration can be checked by viewing the displayed Smith Chart for the probe measurement in air and with the shorting block. A quick indicator for a calibration that was correctly performed shows for both air and shorting block the plotted line (probe response) running along the outer edge of the Smith Chart in opposite directions.

4.2 Load Selection for Network Analyzer Calibration

The standard method for calibration of a network analyzer is to make 3 calibration measurements using an attachment providing an open-circuit, a short-circuit and a 50 ohm load whose theoretical reflection coefficients are 1, -1 and 0, respectively. When using the open-ended probe, the 50 ohm load is replaced by a liquid dielectric that provides the 'load' for calibration. We considered a number of liquids varying in dielectric that might be used as load. We determined the error of calibration by re-measuring the load and open-circuit (air) after calibration and subtracting the measured spectra from the expected values of 0 and 1, respectively. In Figure 14 the smallest total root mean squared error is associated with the 50 ohm load (i.e., no probe attached to cable). The next lowest error was from ethylene glycol (antifreeze) followed by water. Note the dioxane errors were an order of magnitude larger than the values shown.

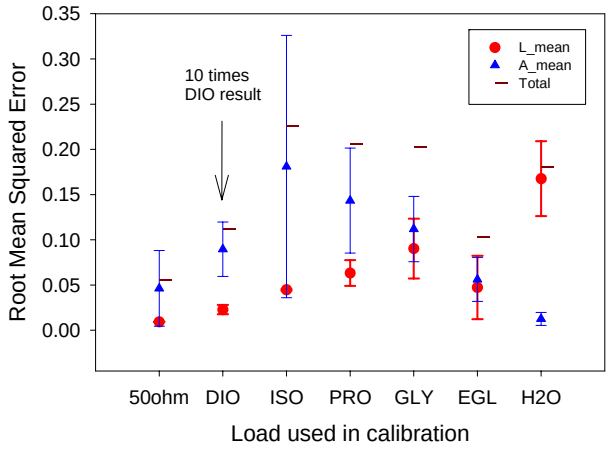

Figure 14. Root mean squared errors associated with use of various loads in the Anritsu Network Analyzer calibration. The load mean (L_mean) and air mean (A_mean) or open-circuit are added together to obtain the total error. The 50 ohm load is the standard, DIO is dioxane, ISO is 2-isopropoxyethanol, PRO is 1-propanol, GLY is glycerin, EGL is ethylene glycol and H2O is water.

4.3 Bilinear Analysis of Dielectric Liquid Measurements

The bilinear analysis begins with determination of bilinear coefficients described in Eq. (11)

using two known dielectric liquids. The resulting coefficients then become an integral part of computing dielectric spectra for other materials. The coefficients are solved for using a system of linear equations, where the measured scatter functions for the two bilinear analysis reference liquids (BARL) are standardized with respect to the reference scatter function (Γ_{ref}) measured in air using a modified reflection coefficient expression [*Folgerø and Tjomsland*, 1996]

$$\rho^*_{SF} = \frac{\Gamma_{ref} - \Gamma_m}{\Gamma_{ref} + \Gamma_m} \tag{14}$$

where Γ_m is the measured scatter function. In the paper by Folgero and Tjomsland (1996), they used a known liquid as the reference, but we have used air as the reference since it provides an upper bound on the scatter function shown in Figure 15. We found Eq. (11) more difficult to apply to bilinear analysis than a TDR-based version presented by Cole (1983).

$$\varepsilon_x * = \frac{(1 + A^*(\omega))\rho^*_{SF}(\omega)}{1 - B^*(\omega)\rho^*_{SF}(\omega)} \tag{15}$$

In this equation, the parameter C reportedly varied between 0 and 1 and was ignored in their analysis. In order to determine parameters A and B, a set of equations were solved simultaneously, where ρ^*_{SF} is the frequency-dependant standardized scatter function of the BARL. The set of equations are written

$$A^* \rho_1^* + \varepsilon_{x1}^* B^* \rho_1^* = \varepsilon_{x1}^* - \rho_1^*$$
$$A^* \rho_2^* + \varepsilon_{x2}^* B^* \rho_2^* = \varepsilon_{x2}^* - \rho_2^* \quad (16)$$

where ρ_1^* and ρ_2^* are the two measured standardized reflection coefficients of the BARL. These are plotted in Figure 16 for Isopropoxyethanol – water (I:W) mixtures of 0.68 and 0.92. The complex permittivities (ε_x^*) of the two calibration liquids were defined in terms of their Cole-Cole parameters. The parameters are listed in Table 1 and the permittivities are plotted in Figure 16. After the solution of Eq. (15) the bilinear coefficients can be shown to be a function of frequency and uniquely determined by the load-calibration liquid-probe-cable-network analyzer system. If any component is changed, a new calibration must be carried out. These parameters are plotted in Figure 17, illustrating the role that they play in filtering out noise resulting from component imperfections, impedance mismatch, and other anomalies.

4.4 Bilinear Analysis Validation

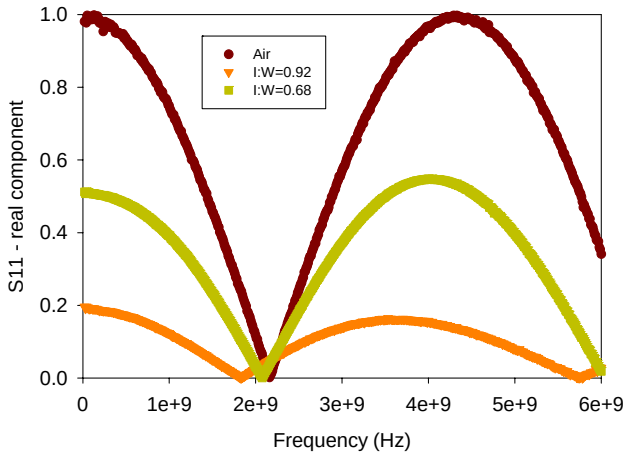

Figure 15. Real component of the scatter function, S11, for air and two bilinear analysis reference liquids (BARL).

With the bilinear coefficients determined, the network analyzer and dielectric probe can be used to measure unknown dielectric materials. Before doing so, we validate the calibration by simply plotting the Cole-Cole specified real permittivity against the calculated permittivity of the two reference dielectrics using bilinear analysis, shown in Figure 16. We also plotted real permittivities of several other liquids measured using the BARL derived parameters (A and B) and compared these to the modeled results from Jones et al., (2005). The complete set of test liquids are shown in Figure 18 where the shift in relaxation frequency is a result of our measurements being made at different temperature (27 C) than those of Jones et al. (2005; 24 C). The goodness of fit within the range of typical soil permittivities in the field is very good. Note that the relaxation frequency of these liquids is relatively high except for

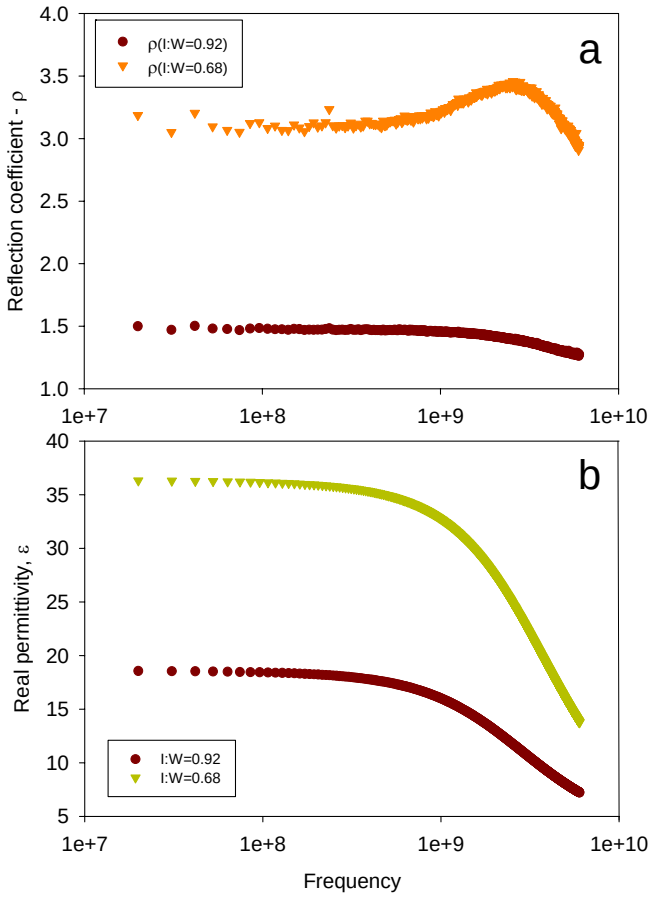

Figure 16. a) Standardized reflection coefficient (ρ) of the two bilinear analysis reference liquids (BARL) as a function of frequency. b) Real permittivities (ε) of the BARL obtained from bilinear analysis.

propanol, which we included to show lower relaxation response.

4.5 Soil Water Content Determination

The calibrated open-ended probe was used to measure the reflection coefficient of a variably-saturated silt loam soil. Using the pressurized soil test apparatus described previously, the silt loam soil was packed air dry into the modified Tempe cell shown in Figure 19. The cell was initially subjected to a vacuum while water was applied from the bottom through the ceramic plate to wet the sample and minimize air entrapment. Once saturated, measurements from the open-ended

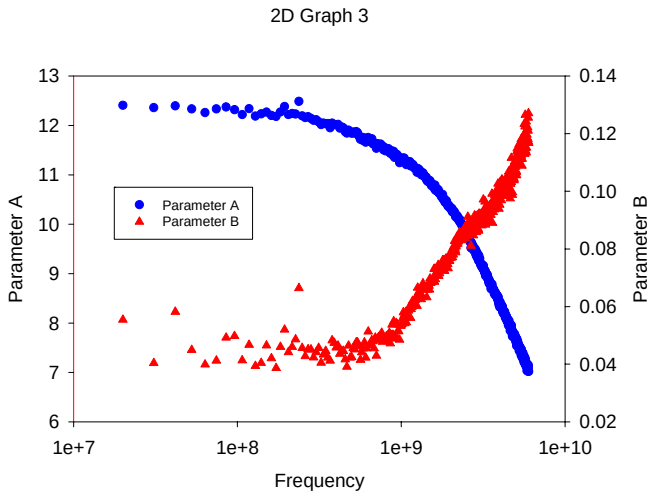

Figure 17. Frequency-dependent bilinear coefficients derived from the two calibration liquids illustrated in Figure 16

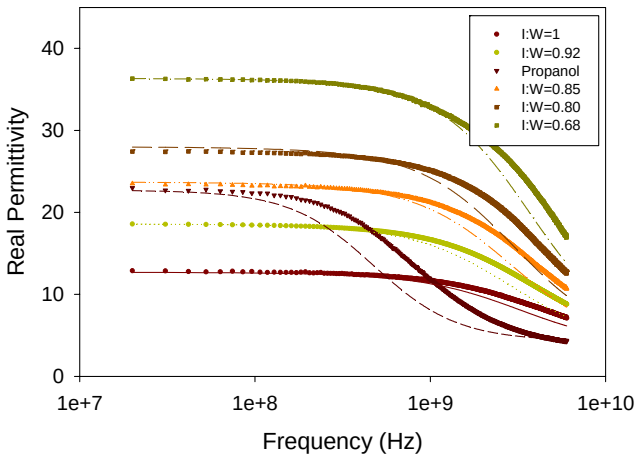

Figure 18. Real permittivity of different dielectric liquids where symbols are the derived values obtained from bilinear analysis and the lines are debye modeled values based on the reference network analyzer measurements. Liquids used are propanol and mixtures of isopropoxyethanol and water where the number indicates the percentage of alcohol in the mixture. The shift in relaxation frequency between reference and measurement is due to differences in sample temperature.

probe and EC-5 sensor were recorded and the first pressure step was applied. The subsequent pressure steps and measured water contents are plotted in Figure 19 where a previously fitted retention curve for the soil is shown for comparison.

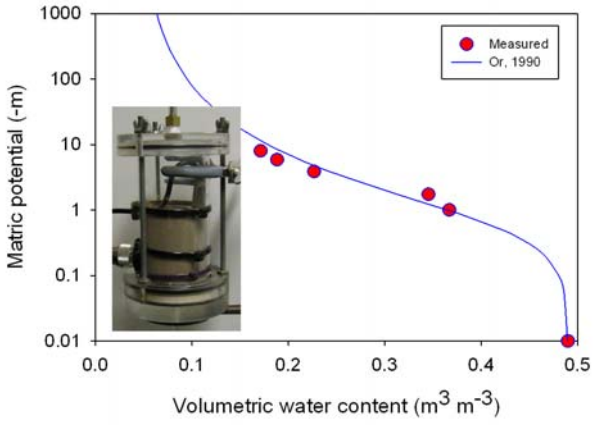

Figure 19. Soil water retention of Milville Silt Loam soil described using modeled results from Or [1990] using the van Genuchten [1980] parameters compared to the modified Tempe cell measured values. The Tempe Cell partially filled with soil is inset in the figure.

Measurements from the N-type open-ended probe installed in the cell were made in air, water and after packing the air-dry soil in the cell. The reflection coefficients measured using the portable network analyzer were stored. The discrete data were standardized using Eq. (14), which was then inserted to Eq. (15) for calculation of the complex permittivity. The real and imaginary permittivities of the variably saturated silt loam soil are plotted in Figure 20, showing considerable relaxation, especially at the lower frequency range. The designations shown in the figure refer to the matric potential imposed by each pressure setting in the cell. These data values are assumed to be the matric potential-water content of the soil at equilibrium.

The soil volumetric water content is best calibrated to permittivity readings using independent measurements of water content by oven drying samples. Another option is to assume a permittivity-soil water content relationship using a volumetric mixing model [*Dirksen and Dasberg*, 1993; *Friedman*, 1998; *Sihvola*, 1997]or empirical equation [*Robinson et al.*, 2005a; *Roth et al.*, 1992; *Topp et al.*, 1980]. The difficulty in resolving the volumetric water content from permittivity measurements in the frequency domain comes from relaxation effects which result in varying permittivity with frequency. A method suggested by Or and Rasmussen [1999] to obtain the effective measurement frequency compares TDR-based permittivity determination with network analyzer measurements indicating the effective frequency as corresponding with the TDR-determined permittivity value. We provide a comparison here by simply taking several discrete frequency-dependent permittivities and computing volumetric water contents (VWC) based on the Topp et al., (1980) equation given as

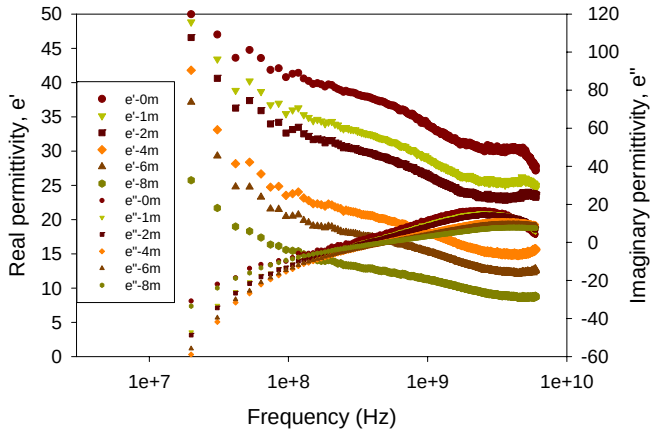

Figure 20. Frequency-dependent real (large symbols) and imaginary (smaller symbols) permittivities of Milville Silt Loam soil at varied matric potentials. Readings are derived from bilinear analysis using network analyzer measurements.

$$VWC = -5.3x10^{-2} + 2.92x10^{-2}\varepsilon_b - 5.5x10^{-4}\varepsilon_b^{\,2} + 4.3x10^{-6}\varepsilon_b^{\,3} \qquad (17)$$

where ε_b is the bulk dielectric permittivity, which we replace with the real permittivity to obtain an estimate of water content shown in Figure 21. For the range of matric potential induced water contents shown, the 'Cell' water contents correspond to a frequency of 0.5 GHz at saturation and to a 5 GHz frequency at the lowest water content. It is unclear why the intermediate water contents determined by the cell measurements fall below all frequencies of the network analyzer. The EC-5 sensor readings show a similar, though offset pattern compared with the bulk volumetric water content of the cell based on mass balance calculations. The discrepancy between the bulk cell water content and those inferred from the open-ended probe measurements in the bottom half of the cell is unclear. It is possible that there was some

separation of the sample from the open-ended probe surface upon drying in this shrinkage prone soil. The apparent enhancement in water content would suggest there was a water-filled gap, which is unlikely during a drainage process in which larger pores tend to drain first. The greater correlation of water content near saturation for 0.5 GHz is consistent with results found using TDR, where the effective measurement frequency is up to 1.5 GHz [*Heimovaara et al.*, 1996; *Robinson et al.*, 2005b]. Further measurements are needed to identify the nature of the discrepancy whether experimental error or other phenomena.

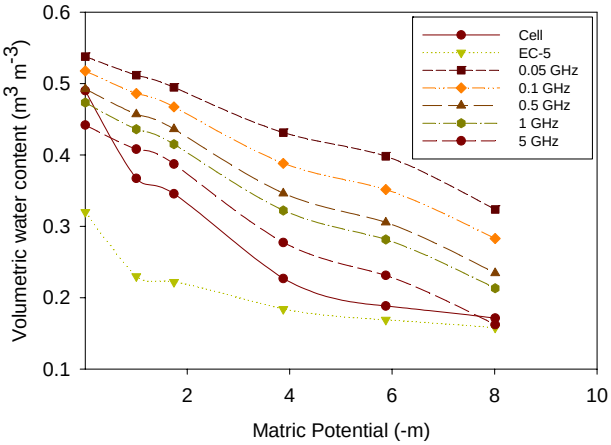

Figure 21. Volumetric water content values derived from Tempe Cell measurements, the EC-5 sensor, and from the Topp et al., (1980) equation using discrete frequency-dependent permittivity measurements of Network Analyzer.

4.6 Future Research Needs

The opportunity to measure frequency-dependent permittivity of soil and other porous materials has tremendous potential to provide details regarding soil properties. These properties include soil texture, soil salinity, soil aggregation and other factors which influence dielectric-permittivity, -loss and -relaxation within the measured frequency spectrum. As the cost of instrumentation is reduced, full spectra

measurements will become routinely available and researchers will begin expanding model and prediction capabilities for interpretation of measured spectra. Future frequency domain permittivity measurements will be coupled with infrared and optical measurements of soil properties to enhance the information content of precision agriculture. Before reaching this level of advancement, significant effort is needed to develop more affordable measurement techniques, improve prediction capability and develop robust approaches for determination of soil properties. Techniques for obtaining frequency spectra using time domain reflectometry have been demonstrated through fast Fourier transformation of the waveform [*Friel and Or*, 1999; *Heimovaara*, 1994; *Jones and Or*, 2004]. Such an approach would reduce costs significantly over network analyzer measurements. Although there have been studies which measured soil permittivity spectra in soils, a significant database is needed from which to develop model and prediction capabilities. Dielectric permittivity databases developed around soils already incorporated in pedotransfer functions for example may improve prediction capabilities overall when combined. While electromagnetic soil moisture sensors are probably adequate for long-term monitoring when calibrated, there is a significant need for on-the-go measurement capabilities in soils with unknown dielectric-water content relationships. Patents or patent applications exist that describe mobile subsurface water content measurement systems [*Schuler et al.*, 2003; *Shibusawa et al.*, 2005] but with little information on the accuracy of measurement. Stop and go

systems requiring TDR probes to be inserted and removed at each location have been developed and evaluated [*Thomsen et al.*, 2005; *Wraith et al.*, 2005]. Little however has appeared in the scientific literature regarding reliable and accurate water content sensing capability for on-the-go mapping. The need for mobile measurement capabilities is expressed in field-scale mapping of soil used in precision agriculture, soil excavation and construction activities, military activities taking place in unknown terrain, large-scale calibration of remotely sensed soil moisture and other needs requiring mobile measurements of permittivity for water content determination. We see many opportunities to complement precision agriculture with mobile water content measurement using open-ended dielectric probes embedded in a plow or other implement pulled through the soil. There are no doubt challenges to implementation of such a sensor including surface wear, soil compaction effects, particle/aggregate size effects and maintenance of soil-probe contact.

5. Conclusions

We have suggested frequency-domain measurements of permittivity for water content determination as an improvement in the information content related to soil-specific properties that influence the permittivity spectra. Such measurements are likely to provide information related to the soil texture and salinity that are unavailable from conventional EM sensor measurements (i.e., from single, fixed frequency

measurements). A portable network analyzer and custom-made dielectric probe were coupled with bilinear analysis of the network analyzer output to obtain permittivity spectra in liquids. Measurements were well correlated with a commercial system measurement of permittivity across a range of dielectric liquids. Liquid dielectrics were mixtures of alcohols and water.

In developing the approach, the quality of the calibration was found to be a critical step for obtaining accurate permittivity determinations. The probe is first calibrated using an open, short-circuit and load, where the load plays a key role in the quality of measurement. We found water to be among the best 'readily available' loads to use as the load. The short-circuit is a key calibration measurement and must be obtained with highly polished, smooth surfaces (i.e., probe and metal foil). A range of permittivities were evaluated to determine the optimal bilinear analysis reference liquids (BARL) for calibration, finding that the optimal permittivities are generally at the upper and lower range of interest (e.g., for soil between 5 and 40).

A pressure cell was constructed for permittivity measurements in a silt loam soil with varied volumetric water content. By tracking cell water outflow across a pressure step range from 0 to 8 m of pressure head, the volumetric water content of the sample at each step was determined. We used the Topp et al., (1980) relationship commonly employed in time domain reflectometry measurements to volumetric water content

from the real permittivity derived from the portable network analyzer and bilinear analysis. These preliminary results showed an effective frequency at saturation near 0.5 GHz (i.e., water contents were correlated) but the correlations diverged with reducing water content where the cell values fell below all NA-derived values. Only at the driest point did the correlation return with an effective frequency of 1 GHz being common. Further testing will look for possible experimental deficiencies in the measurement approach. We expect to find better consistency in the effective measurement frequency for varied water content of the sample.

6. References

Aralaguppi, M. I., et al. (1996), Density, Refractive Index, Viscosity, and Speed of Sound in Binary Mixtures of 2-Ethoxyethanol with Dioxane, Acetonitrile, and Tetrahydrofuran at (298.15, 303.15, and 308.15) K, *J. Chem. Eng. Data*, *41*(6), 1307-1310.

Berberian, J. G. (1993), Time domain reflectometry: Bilinear corrections and extending the range of analysis beyond the quarter and half wavelength conditions, *J Mol. Liquids*, *56*, 1-18.

Blonquist, J. M., Jr., et al. (2005), Standardizing Characterization of Electromagnetic Water Content Sensors: Part 2. Evaluation of Seven Sensing Systems, *Vadose Zone J*, *4*(4), 1059-1069.

Bogena, H. R., et al. (2007), Evaluation of a low-cost soil water content sensor for wireless network applications, *Journal of Hydrology*, *344*(1-2), 32-42.

Chen, y., and D. Or (2006), Effects of Maxwell-Wagner polarization on soil complex dielectric permittivity under variable temperature and electrical conductivity, *Wat. Resour. Res.*, *42*(6), W06424.

Cole, K. S., and R. H. Cole (1941), Dispersion and adsorption in dielectrics: I--Alternating current characteristics, *J. Chem. Phys.*, *9*, 341-351.

Cole, R. H. (1983), Bridge Sampling Methods for Admittance Measurements from 500 kHz to 5 GHz, *IEEE Transactions on Instrumentation and Measurement*, *32*(1), 42-47.

Cole, R. H., et al. (1989), Time domain reflection methods for dielectric measurements to 10 GHz, *J. Appl. Phys.*, *66*(2), 793-802.

De Langhe, P., et al. (1994), Design rules for an experimental setup using an open-ended coaxial probe based on theoretical modelling, *IEEE Transactions on Instrumentation and Measurement*, *43*(6), 810-817.

Dirksen, C., and S. Dasberg (1993), Improved calibration of time domain reflectometry soil water content measurements, *Soil Sci. Soc. Am. J.*, *57*, 660-667.

Folgerø, K., and T. Tjomsland (1996), Permittivity measurements of thin liquid layers using open-ended coaxial probes, *Meas. Sci. Technol.*, *7*, 1164-1173.

Friedman, S. P. (1998), A saturation degree-dependent composite spheres model for describing the effective dielectric constant of unsaturated porous media, *Water Resour. Res.*, *34*(11).

Friel, R., and D. Or (1999), Frequency analysis of time-domain reflectometry (TDR) with application to dielectric spectroscopy of soil constituents, *Geophysics*, *64*(3), 1-12.

Grant, J. P., et al. (1989), A critical study of the open-ended coaxial-line sensor technique for RF and microwave complex permittivity measurements *J. Phys. E: Sci. Instrum.*, *22*, 757-770.

Hasted, J. B. (1973), *Aqueous Dielectrics*, 302 pp., John Wiley & Sons, New York.

Heimovaara, T. J. (1994), Frequency domain analysis of time domain reflectometry waveforms: 1. Measurement of the complex dielectric permitivity of soils., *Water Resour. Res.*, *30*(2), 189-199.

Heimovaara, T. J., et al. (1996), Frequency-dependent dielectric permittivity from 0 to 1 GHz: Time domain reflectometry measurements compared with frequency domain network analyzer measurements., *Water Resour. Res.*, *32*(12), 3603-3610.

Jones, S. B., and D. Or (2004), Frequency Domain Analysis for Extending Time Domain Reflectometry Water Content Measurement in Highly Saline Soils, *Soil Sci. Soc. Am. J.*, *68*(5), 1568-1577.

Jones, S. B., et al. (2005), Standardizing Characterization of Electromagnetic Water Content Sensors: Part 1. Methodology, *Vadose Zone J*, *4*(4), 1048-1058.

Jones, S. B., et al. (2006), Development of a subsurface open-ended TDR probe for on-the-go mapping of water content, in *Proc. 3rd International Symposium and Workshop on Time Domain Reflectometry for Innovative Soils Applications*, edited, p. Paper 17, Purdue University, Purdue University, West Lafayette, USA.

Or, D. (1990), Irrigation management considering soil variability and climatic uncertainty, 224 pp, Utah State University, Logan.

Or, D., and V. P. Rasmussen (1999.), Effective frequency of TDR travel time-based measurement of bulk dielectric permittivity paper presented at Third Workshop on Electromagneitic Wave Interaction with Water and Moist Substances, Athens, GA., 12-13 Apr.

Robinson, D. A., et al. (2005a), A Physically Derived Water Content/Permittivity Calibration Model for Coarse-Textured, Layered Soils, *Soil Sci. Soc. Am. J.*, *69*(5), 1372-1378.

Robinson, D. A., et al. (2005b), On the Effective Measurement Frequency of TDR in Dispersive and Non-Conductive Dielectric Materials, *Water Resour. Res.*, *41*(2), W02007.

Roth, C. H., et al. (1992), Empirical evaluation of the relationship between soil dielectric constant and volumetric water content as the basis for calibrating soil moisture measurements by TDR, *J. Soil Sci.*, *43*.

Schuler, R. T., et al. (2003), Soil Moisture Measuring System for a Mobile Agricultural Device, edited by U. S. P. Application.

Schwank, M., et al. (2006), Laboratory Characterization of a Commercial Capacitance Sensor for Estimating Permittivity and Inferring Soil Water Content, *Vadose Zone J*, *5*(3), 1048-1064.

Sheen, N. I., and I. M. Woodhead (1999), An Open-ended Coaxial Probe for Broad-band Permittivity Measurement of Agricultural Products, *J. agric. Engng Res.*, *74*, 193-202.

Shibusawa, S., et al. (2005), Soil characteristics survey device and soil characteristic survey method, edited by U. S. Patent, USA.

Sihvola, A. (1997), A review of dielectric mixing models, Helsinki University of Technology; Dept. of Electrical and Communications Engineering, Helsinki.

Smith-Rose, R. L. (1933), The Electrical Properties of Soil for Alternating Currents at Radio Frequencies, *Proceedings of the Royal Society of London. Seires A.*, *140*(841), 359-377.

Stuchly M. A., S. S. S. (1982), Measurement of Radio Frequency Permittivity of Biological Tissues with an Open-Ended Coaxial Line: Part I, *IEEE Transactions on Microwave Theory and Techniques*, *82*(1), 82-86.

Thomsen, A., et al. (2005), Mobile TDR for geo-referenced measurement of soil water content and electrical conductivity, in *Precision Agriculture '05*, edited by J. V. Stafford, pp. 481-494, Wageningen Academic Publishers, Wageningen, The Netherlands.

Topp, G. C., et al. (1980), Electromagnetic determination of soil water content: Measurements in coaxial transmission lines, *Water Resour. Res.*, *16*, 574-582.

vanGenuchten, M. T. (1980), A closed-form equation for predicting the hydraulic conductivity of unsaturated soils, *Soil Sci. Soc. Am. J.*, *44*, 892-898.

Wraith, J. M., et al. (2005), Spatially characterizing apparent electrical conductivity and water content of surface soils with time domain reflectometry, *Computers and Electronics in Agriculture 46*(1-3), 239-262.